

# Efficient planar fiber-to-chip coupler based on two-stage adiabatic evolution

Anatol Khilo,<sup>1,\*</sup> Miloš A. Popović,<sup>2</sup> Mohammad Araghchini,<sup>1</sup> and Franz X. Kärtner<sup>1</sup>

<sup>1</sup>Department of Electrical Engineering and Computer Science and Research Laboratory of Electronics, Massachusetts Institute of Technology, 77 Massachusetts Avenue, Cambridge, MA, 02139, USA

<sup>2</sup>Department of Electrical, Computer and Energy Engineering, University of Colorado, Boulder, CO 80309, USA  
\*anatoly@mit.edu

**Abstract:** A new, efficient adiabatic in-plane fiber-to-chip coupler design is proposed. In this design, the light from the fiber is coupled into a low-index waveguide with matching mode size. The mode is first adiabatically reduced in size with a rib taper, and then transferred into a high-index (e.g. silicon) waveguide with an inverse taper. The two-stage design allows to reduce the coupler length multiple times in comparison with pure inverse taper-based couplers of similar efficiency. The magnitude of length reduction increases with the refractive index of the low-index waveguide and the fiber mode size.

©2010 Optical Society of America

OCIS codes: (130.0130) Integrated optics; (130.3120) Integrated optics devices.

---

## References and links

1. R. Orobtcouk, "On Chip Optical Waveguide Interconnect: the Problem of the In/Out Coupling," in *Optical Interconnects: the Silicon Approach*, L. Pavesi, G. Guillot, eds. (Springer, 2006).
2. Y. Shani, C. H. Henry, R. C. Kistler, K. J. Orlowsky, and D. A. Ackerman, "Efficient coupling of a semiconductor laser to an optical fiber by means of a tapered waveguide on silicon," *Appl. Phys. Lett.* **55**(23), 2389–2391 (1989).
3. T. Shoji, T. Tsuchizawa, T. Watanabe, K. Yamada, and H. Morita, "Low loss mode size converter from 0.3 $\mu$ m square Si wire waveguides to singlemode fibres," *Electron. Lett.* **38**(25), 1669–1670 (2002).
4. T. Tsuchizawa, K. Yamada, H. Fukuda, T. Watanabe, Jun-ichi Takahashi, M. Takahashi, T. Shoji, E. Tamechika, S. Itabashi, and H. Morita, "Microphotonics Devices Based on Silicon Microfabrication Technology," *IEEE J. Sel. Top. Quantum Electron.* **11**(1), 232–240 (2005).
5. S. McNab, N. Moll, and Y. Vlasov, "Ultra-low loss photonic integrated circuit with membrane-type photonic crystal waveguides," *Opt. Express* **11**(22), 2927–2939 (2003), <http://www.opticsinfobase.org/abstract.cfm?URI=oe-11-22-2927>.
6. V. R. Almeida, R. R. Panepucci, and M. Lipson, "Nanotaper for compact mode conversion," *Opt. Lett.* **28**(15), 1302–1304 (2003).
7. G. Roelkens, P. Dumon, W. Bogaerts, D. Van Thourhout, and R. Baets, "Efficient silicon-on-insulator fiber coupler fabricated using 248-nm-deep UV lithography," *IEEE Photon. Technol. Lett.* **17**(12), 2613–2615 (2005).
8. K. K. Lee, D. R. Lim, D. Pan, C. Hoepfner, W.-Y. Oh, K. Wada, L. C. Kimerling, K. P. Yap, and M. T. Doan, "Mode transformer for miniaturized optical circuits," *Opt. Lett.* **30**(5), 498–500 (2005).
9. D. Taillaert, W. Bogaerts, P. Bienstman, T. F. Krauss, P. Van Daele, I. Moerman, S. Verstuyft, K. De Mesel, and R. Baets, "An out-of-plane grating coupler for efficient butt-coupling between compact planar waveguides and single-mode fibers," *IEEE J. Quantum Electron.* **38**(7), 949–955 (2002).
10. D. Taillaert, P. Bienstman, and R. Baets, "Compact efficient broadband grating coupler for silicon-on-insulator waveguides," *Opt. Lett.* **29**(23), 2749–2751 (2004).
11. B. Wang, J. Jiang, D. M. Chambers, J. Cai, and G. P. Nordin, "Stratified waveguide grating coupler for normal fiber incidence," *Opt. Lett.* **30**(8), 845–847 (2005).
12. F. Van Laere, G. Roelkens, M. Ayre, J. Schrauwen, D. Taillaert, D. Van Thourhout, T. F. Krauss, and R. Baets, "Compact and Highly Efficient Grating Couplers Between Optical Fiber and Nanophotonic Waveguides," *J. Lightwave Technol.* **25**(1), 151–156 (2007).
13. M. Fan, M. Popović, and F. X. Kärtner, "High Directivity, Vertical Fiber-to-Chip Coupler with Anisotropically Radiating Grating Teeth," in *Conference on Lasers and Electro-Optics/Quantum Electronics and Laser Science*, Technical Digest (CD) (Optical Society of America, 2007), paper CTuDD3.
14. I. E. Day, I. Evans, A. Knights, F. Hopper, S. Roberts, J. Johnston, S. Day, J. Luff, H. K. Tsang, and M. Asghari, "Tapered Silicon Waveguides for Low Insertion Loss Highly-Efficient High-Speed Electronic Variable Optical Attenuators," in *Optical Fiber Communication Conference*, Technical Digest (CD) (Optical Society of America, 2003), paper TuM5.
15. R. J. Bozeat, S. Day, F. Hopper, F. P. Payne, S. W. Roberts, and M. Asghari, "Silicon Based Waveguides," in *Silicon Photonics*, L. Pavesi, D. J. Lockwood, eds. (Springer, 2004).

16. T. Aalto, K. Solehmainen, M. Harjanne, M. Kapulainen, and P. Heimala, "Low-loss converters between optical silicon waveguides of different sizes and types," *IEEE Photon. Technol. Lett.* **18**(5), 709–711 (2006).
17. J. K. Doylend, and A. P. Knights, "Design and Simulation of an Integrated Fiber-to-Chip Coupler for Silicon-on-Insulator Waveguides," *IEEE J. Sel. Top. Quantum Electron.* **12**(6), 1363–1370 (2006).
18. A. Barkai, A. Liu, D. Kim, R. Cohen, N. Elek, H. Chang, B. H. Malik, R. Gabay, R. Jones, M. Paniccia, and N. Izhaky, "Double-Stage Taper for Coupling Between SOI Waveguides and Single-Mode Fiber," *J. Lightwave Technol.* **26**(24), 3860–3865 (2008).
19. D. Dai, S. He, and H. Tsang, "Bilevel Mode Converter Between a Silicon Nanowire Waveguide and a Larger Waveguide," *J. Lightwave Technol.* **24**(6), 2428–2433 (2006).
20. K. Shiraiishi, H. Yoda, A. Ohshima, H. Ikedo, and C. S. Tsai, "A silicon-based spot-size converter between single-mode fibers and Si-wire waveguides using cascaded tapers," *Appl. Phys. Lett.* **91**(14), 141120 (2007).
21. A. Sure, T. Dillon, J. Murakowski, C. Lin, D. Pustai, and D. Prather, "Fabrication and characterization of three-dimensional silicon tapers," *Opt. Express* **11**(26), 3555–3561 (2003), <http://www.opticsinfobase.org/abstract.cfm?URI=oe-11-26-3555>.
22. M. Fritze, J. Knecht, C. Bozler, C. Keast, J. Fijol, S. Jacobson, P. Keating, J. LeBlanc, E. Fike, B. Kessler, M. Frish, and C. Manolatos, "Fabrication of three-dimensional mode converters for silicon-based integrated optics," *J. Vac. Sci. Technol. B* **21**(6), 2897–2902 (2003).
23. C. Manolatos, and H. A. Haus, *Passive components for dense optical integration* (Kluwer Academic Publishers, 2001), chap. 6.
24. V. Nguyen, T. Montalbo, C. Manolatos, A. Agarwal, C. Hong, J. Yasaitis, L. C. Kimerling, and J. Michel, "Silicon-based highly-efficient fiber-to-waveguide coupler for high index contrast systems," *Appl. Phys. Lett.* **88**(8), 081112 (2006).
25. R. Sun, V. Nguyen, A. Agarwal, C. Hong, J. Yasaitis, L. Kimerling, and J. Michel, "High performance asymmetric graded index coupler with integrated lens for high index waveguides," *Appl. Phys. Lett.* **90**(20), 201116 (2007).
26. A. Khilo, M. Popović, and F. X. Kärtner, "Efficient Planar Fiber-to-Chip Coupler based on Two-Stage Adiabatic Evolution," presented at ICONO/LAT Conference, Minsk, Belarus, 2007, paper IO2/VIII-1.
27. A. Khilo, and F. X. Kärtner, "Efficient Planar Single-Mode Fiber-to-Chip Coupler based on Two-Stage Adiabatic Evolution," in *Conference on Lasers and Electro-Optics/Quantum Electronics and Laser Science*, Technical Digest (CD) (Optical Society of America, 2010), paper JThE30.
28. Q. Fang, T.-Y. Liow, J. F. Song, C. W. Tan, M. B. Yu, G. Q. Lo, and D.-L. Kwong, "Suspended optical fiber-to-waveguide mode size converter for silicon photonics," *Opt. Express* **18**(8), 7763–7769 (2010), <http://www.opticsinfobase.org/abstract.cfm?URI=oe-18-8-7763>.
29. M. Qi, M. R. Watts, T. Barwicz, L. Socci, P. Rakich, E. P. Ippen, and H. I. Smith, "Fabrication of Two-Layer Microphotonic Structures without Planarization," in *Conference on Lasers and Electro-Optics/Quantum Electronics and Laser Science*, Technical Digest (CD) (Optical Society of America, 2005), paper CWD5.
30. T. Barwicz, M. R. Watts, M. A. Popovic, P. T. Rakich, L. Socci, F. X. Kärtner, E. P. Ippen, and H. I. Smith, "Polarization-transparent microphotonic devices in the strong confinement limit," *Nat. Photonics* **1**(1), 57–60 (2007).
31. M. A. Popović, T. Barwicz, E. P. Ippen, and F. X. Kärtner, "Global design rules for silicon microphotonic waveguides: sensitivity, polarization and resonance tunability," in *Conference on Lasers and Electro-Optics/Quantum Electronics and Laser Science*, Technical Digest (CD) (Optical Society of America, 2006), paper CTuCC1.
32. FIMMWAVE/FIMMPROP by Photon Design, <http://www.photond.com>.
33. C. W. Holzwarth, J. S. Orcutt, H. Li, M. A. Popović, V. Stojanović, J. L. Hoyt, R. J. Ram, and H. I. Smith, "Localized Substrate Removal Technique Enabling Strong-Confinement Microphotonic in Bulk Si CMOS Processes," in *Conference on Lasers and Electro-Optics/Quantum Electronics and Laser Science*, Technical Digest (CD) (Optical Society of America, 2008), paper CThKK5.
34. S. Selvaraja, P. Jaenen, W. Bogaerts, D. VanThourhout, P. Dumon, and R. Baets, "Fabrication of Photonic Wire and Crystal Circuits in Silicon-on-Insulator Using 193-nm Optical Lithography," *J. Lightwave Technol.* **27**(18), 4076–4083 (2009).
35. T. Barwicz, M. A. Popović, M. R. Watts, P. T. Rakich, E. P. Ippen, and H. I. Smith, "Fabrication of Add-Drop Filters Based on Frequency-Matched Microring Resonators," *J. Lightwave Technol.* **24**(5), 2207–2218 (2006).
36. T. Barwicz, and H. A. Haus, "Three-Dimensional Analysis of Scattering Losses Due to Sidewall Roughness," *J. Lightwave Technol.* **23**(9), 2719–2732 (2005).

---

## 1. Introduction

Integrated circuits using strongly-confining waveguides are promising for implementation and dense integration of high-performance microphotonic components on a chip. The optical input is usually generated outside the chip and is transmitted onto the chip through an optical fiber. However, coupling of light between the fiber and a sub-micron strong-confinement waveguide is not a trivial task because of the enormous mode mismatch between them. For instance, the mode area needs to be reduced several hundred times for coupling light from a standard single-mode fiber into a sub-micron silicon waveguide. This paper proposes a new,

two-section planar coupler design that transforms the mode from a fiber to a sub-micron strong-confinement waveguide with high efficiency and a reduced footprint on the chip.

A number of solutions for coupling light between optical fibers and submicron strong-confinement waveguides have been developed [1]. These solutions can be categorized into in-plane and out-of-plane, depending on whether or not the optical fiber is located in the same plane with the optical chip. The most prominent in-plane and out-of-plane couplers are probably the inverse taper-based and grating-based couplers, respectively.

In couplers based on inverse tapers, the light from the fiber is first coupled into an intermediate waveguide with a mode size matching that of the fiber. This waveguide is sometimes called the low index waveguide, because the index contrast between its core and undercladding is much lower than the index contrast of a strong-confinement (e.g. silicon) waveguide. An inverse high-index taper is then introduced inside the low-index waveguide. In the inverse taper, the high-index waveguide is very narrow in the beginning so that the fundamental mode is not confined to its core and virtually matches the mode of the low-index guide. The high-index waveguide is then adiabatically widened until the fundamental mode of the structure becomes well-confined in the high-index core. Inverse tapers have previously been used for coupling light between fibers and semiconductor lasers [2], and later the same concept was applied to Si waveguides [3–8]. Shoji and colleagues achieved 0.8dB coupling loss between a fiber with  $4.3\mu\text{m}$  mode size and a  $0.3\times 0.3\mu\text{m}$  Si waveguide [3]. They later reduced the loss to 0.5dB by perfecting the fabrication and using a better material for the low-index waveguide [4]; the coupler length was more than  $200\mu\text{m}$ . A coupling loss of 2.5dB was measured for a standard fiber with  $9\mu\text{m}$  mode. In the work of McNab and colleagues [5], 0.5dB coupling loss has been reported between a microlensed fiber with  $2.1\mu\text{m}$  beam diameter and a  $0.45\times 0.22\mu\text{m}$  Si waveguide with  $150\mu\text{m}$  inverse taper length; the measurement uncertainty was 0.4dB. In the work of Almeida and colleagues [6], a compact  $40\mu\text{m}$ -long inverse taper with parabolic width profile has been proposed, with theoretical coupling loss of about 0.5dB for the TE mode. Because the inverse taper did not have a fiber-matched low-index waveguide on top of it, high efficiency could not be achieved for TE and TM modes simultaneously; in addition, the coupling efficiency was sensitive to errors in Si tip width, because the diameter of the deconfined mode at the tip is strongly dependent on small changes in its width. The experimental coupling loss for a fiber with  $\sim 5\mu\text{m}$  mode field diameter was 3.3dB for TE and 6.0dB for TM modes. While the other works mentioned above relied on e-beam lithography for coupler fabrication, in [7] and [8] the coupler was made with CMOS fabrication tools using 248nm deep UV lithography. In [7], 1dB mode conversion loss and 1.9dB total loss have been demonstrated between a lensed fiber and a sub-micron silicon waveguide with  $3\times 3\mu\text{m}$  overlaying low-index waveguide. In [8], a coupling loss of less than 1dB has been reported between a  $4.5\times 4.5\mu\text{m}$  low-index waveguide and a  $0.4\times 0.7\mu\text{m}$  high-index waveguide with 2.05 refractive index, and  $350\mu\text{m}$  inverse taper.

The second important class of fiber-to-chip couplers is out-of-plane grating-based couplers, in which the light propagating in a waveguide is scattered by a grating; the scattered light is collected by a fiber which is placed in the vertical plane, usually at an angle to the chip normal. An important benefit of vertical couplers is that the light can be coupled in and out at an arbitrary location on the chip, and not only at the chip facet. A number of vertical coupler designs has been proposed and demonstrated [9–13]. To achieve high coupling efficiency, it is necessary to break the top-bottom symmetry of the structure, otherwise the light from the waveguide will be scattered both upwards and downwards. To break the symmetry, a reflector at the bottom of the waveguide can be introduced; 0.4dB coupling loss was predicted for a coupler with a dual-layer Bragg reflector [10], and a coupler with about 1.5dB loss utilizing a gold reflecting layer has been demonstrated [12]. Another way to break the symmetry is to use a two-level grating teeth design [13].

There exists another class of in-plane fiber-to-chip coupler structures where the light from the fiber is coupled into a fiber-matched waveguide with a rib which is adiabatically reduced in width along the coupler in order to shrink the mode size vertically by “squeezing” the mode out from the rib [14–19]. Such structures are usually used for coupling light into rib

waveguides, which is an easier problem than coupling into wire waveguides because the mode size in the former is much larger. In [14,15], the light from a fiber is first coupled into a rib waveguide with matching mode, and then transferred into a rib waveguide with smaller mode size. In [14], the measured coupling loss was less than 0.5dB, the input waveguide rib width was 12 $\mu$ m, and the taper length was 1mm. In [15], a coupling loss of less than 1dB was reported. The fiber mode diameter was 10.4 $\mu$ m, the input fiber-matched rib waveguide was 12.5  $\times$  12.5 $\mu$ m (width  $\times$  height) with 10 $\mu$ m etch depth, the output rib waveguide was 3  $\times$  4 $\mu$ m with 2 $\mu$ m etch depth, and the taper length was about 3mm. In [16], the mode conversion between a 6.8  $\times$  9.4 $\mu$ m rib waveguide and a 2.8  $\times$  3.8 $\mu$ m rib waveguide has been demonstrated with the loss of 0.7  $\pm$  0.2dB; this number did not include the loss due to mode mismatch between the fiber and the rib waveguide. In [17], the upper-layer silicon rib was separated from the lower silicon layer by a thin oxide layer. The effective indices in the upper and the lower layers were matched and light was transferred into the lower layer according to coupled mode theory. This concept eliminates the need to create a very narrow and tall tip at the point where the upper layer is terminated. Simulations predicted less than 0.5dB coupling loss into a sub-micron silicon rib waveguide for a 810 $\mu$ m-long coupler with a 5  $\times$  5 $\mu$ m input Si facet. In [18], a coupler with two ribs with adiabatically decreasing widths has been proposed and fabricated. The introduction of two ribs allowed coupling of light from a standard single-mode fiber rather than from a small-core fiber with reasonable device length. The measured coupling loss from SMF-28 fiber into a 1.5 $\mu$ m-thick silicon rib waveguide was about 1.5dB with a coupler length of 1mm. In [19], it was proposed to use a tapered-rib coupler to couple light directly into a silicon wire waveguide. The simulations predicted 0.5-1dB coupling loss, depending on the height of the output wire waveguide, for a 700 $\mu$ m-long coupler with optimized shape. At the input, the silicon thickness was 4.1 $\mu$ m and the rib width was 2.4 $\mu$ m.

Many other coupler designs have been proposed and demonstrated [20–25]. Many of them rely on complex fabrication techniques to shrink the mode size vertically along the coupler. For example, two cascaded tapers, a horizontal one with varying width and a vertical one with varying thickness, were used in [20] to demonstrate 0.5dB conversion loss from a Si wire waveguide into a 5.1  $\times$  9.2 $\mu$ m mode. The coupler length was about 2mm. Other fabrication efforts of vertical tapers with varying thickness include [21] and [22], with measured coupling losses of 2.2-3.5dB and 16-17dB, respectively. Another approach is to use a graded index layered structure in vertical direction which acts as a lens, combined with a short non-adiabatic taper in horizontal direction [23]. The coupling loss of about 2dB [24] and 0.45 dB [25] has been demonstrated for a 20 $\mu$ m-long coupler.

In this work, we introduce a novel two-stage in-plane coupler design, which combines a rib taper and inverse taper to achieve high mode conversion efficiency [26,27]. It is shown that the two-stage design allows to reduce coupler length at least 2-3 times compared to the pure inverse taper-based coupler of equal efficiency. This allows to couple light from fibers with larger mode size than is possible with inverse taper-based couplers.

In a recent work, a coupler which, similarly to our design, has both a rib taper and an inverse taper has been proposed and demonstrated [28]. The low-index material was SiO<sub>2</sub> itself, with the silicon substrate below it locally removed to form a suspended SiO<sub>2</sub> waveguide. The input 6  $\times$  6 $\mu$ m cross-section of the suspended SiO<sub>2</sub> waveguide was reduced to 2 $\mu$ m horizontally and 5 $\mu$ m vertically using a lateral and a rib taper. After this, a two-layer inverse Si taper was used to convert the mode into Si waveguide. The theoretical loss for a 150 $\mu$ m-long coupler was 0.9dB for TE mode, and the measured loss was 1.7-2.0dB for TE mode and 2.0-2.4dB for TM mode for a lensed fiber with 5 $\mu$ m mode diameter. For a fiber with 9.2 $\mu$ m mode diameter, the loss was 3.8dB for TE mode and 4.0dB for TM mode. Note that although the concept used in [28] is close to the one proposed in our work because it uses both a rib and an inverse taper, there are several important differences. First, our design does not require fabrication of suspended structures and underetching of Si substrate. Second, the rib taper plays a much more prominent role in our design, reducing the vertical extent of the mode by a factor of two or more, while in [28] the vertical size was reduced only from 6 to

5 $\mu$ m. Third, the focus of our work is on understanding the benefits of the two-stage coupler and studying how its performance depends on multiple parameters, while in [28] only one coupler design with fixed parameters has been considered.

The principles of operation of the proposed two-stage coupler are explained in Section 2 and optimization of its parameters is described in Section 3. The performance of the two-stage coupler is analyzed in Section 4. Sections 5 and 6 discuss the choice of the refractive index of the low-index waveguide and the polarization dependence of the coupler, and the concluding Section 7 summarizes the results. Note that while our previous work [27] dealt with single-mode low-index waveguides only, here we present a more general analysis applicable also to the multi-mode case. Throughout the paper, we compare the proposed two-stage design to the design based on pure inverse tapers.

## 2. Concept of the two-stage coupler

The layout of the proposed two-stage coupler is shown in Fig. 1(a). The mode evolution along both stages of the coupler is illustrated in Fig. 1(b). In stage I, the light from the fiber is coupled into a rectangular low-index waveguide with matching mode size. A rib is then introduced in this waveguide. The rib is gradually tapered down along the coupler so that the light is adiabatically transferred into the wider bottom section of the waveguide. When the rib becomes narrow enough, the mode is confined mostly in the wider bottom section of the waveguide, therefore the rib can be terminated at a finite (non-zero) width with very low optical loss. In this way stage I of the coupler, which is referred to as a “rib taper,” adiabatically transfers the optical field from a large fiber-matched rectangular waveguide into a rectangular waveguide of smaller size.

In stage II of the coupler, a high-index inverse taper is introduced inside the low-index waveguide. In this paper we consider silicon as the high-index waveguide material, however, the proposed two-stage coupler concept is expected to be useful also for coupling into other strong-confinement waveguides, such as silicon nitride waveguides. The inverse silicon taper starts from a very narrow tip, so that the mode of the structure is poorly confined in the tip and virtually matches the mode of the lower-index waveguide. The width of the silicon waveguide is then gradually increased so that the mode becomes more and more confined in the Si core, until most of the light is adiabatically transferred from the lower-index into the Si waveguide. At this point the low-index waveguide can be terminated. Stage II of the coupler, which we will also refer to as an “inverse taper,” thus adiabatically converts the fundamental optical mode of the low-index waveguide into the mode of the sub-micron high-index waveguide.

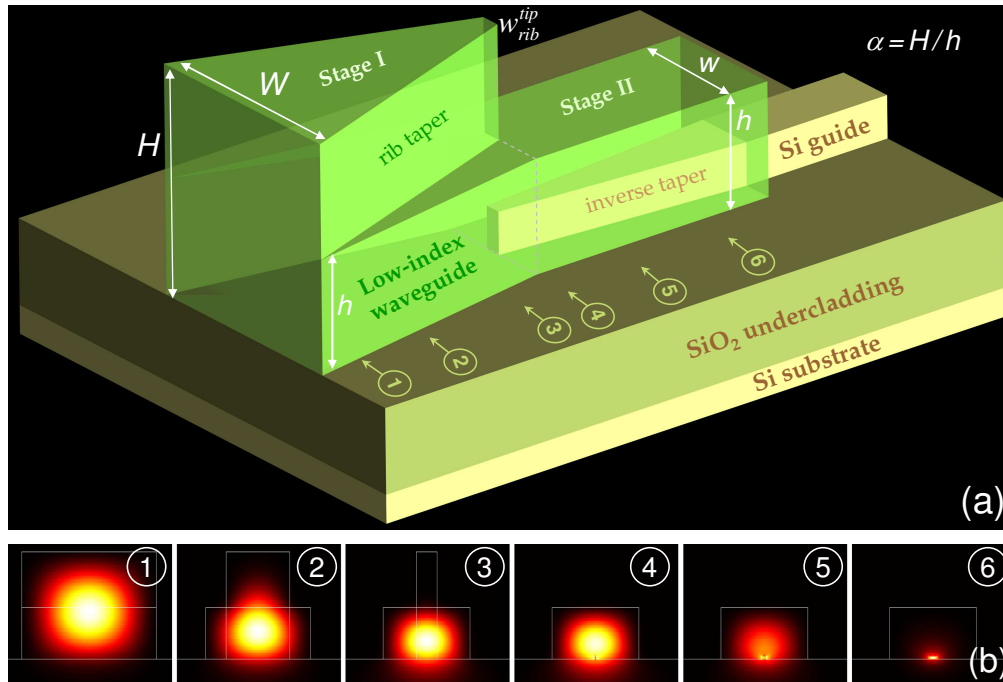


Fig. 1. (a) Layout of the two-stage adiabatic coupler (not drawn to scale). The light from the fiber is coupled into the fiber-matched low-index waveguide, transferred into a smaller waveguide in stage I using a rib taper, and coupled into sub-micron Si waveguide in stage II using an inverse Si taper; (b) intensity distribution of the fundamental TE mode at positions labeled with numbers in Fig. 1(a). Positions 1-3 correspond to the rib taper and 4-6 to the inverse taper.

As described in the introduction, other groups have already used mode converters based on inverse tapers [2–8] as well as rib tapers [14–19]. The inverse taper has been demonstrated to work well for small-core fibers [2–8]. However, as shown in the following section, as the fiber core size increases, the length of the inverse taper required for efficient mode conversion increases rapidly, making the inverse taper-based design impractical for fibers with large cores. Rib tapers easily match to large cores and were demonstrated to be efficient in reducing the mode size several times [14–19], but they cannot reduce the mode size dramatically with realistically short taper lengths. In the proposed two-stage design [26], the rib taper and inverse taper are sharing the mode reduction so that each of them is used efficiently: the rib taper matches to a fiber and reduces the mode size by a moderate amount, and the inverse taper couples the resultant mode into a sub-micron silicon waveguide. As a result, the combination of the two tapers couples light between a fiber and a sub-micron waveguide, overcoming the hundred-fold mode area mismatch with high efficiency and small footprint. Note that a coupler using both a rib and an inverse taper has been a topic of a recent work [28] discussed in the Introduction.

The coupler proposed here can be fabricated as a post-processing step to silicon photonic circuit fabrication, by the deposition of low index layers and a two-step lithography. It should be noted that the two-step lithography can be performed on a single material deposition using dual masks, as previously demonstrated [29,30]. Therefore, we expect that the fabrication complexity of this device is low in comparison to various designs requiring multi-layer fabrication or grayscale lithography, especially relative to the prospective gains in performance.

### 3. Optimization of the two-stage coupler

This section explains the principles of finding the optimal parameters of the two-stage coupler. These principles will be used in the next section to evaluate the performance of the two-stage couplers in general and compare them to the pure inverse taper-based couplers.

Let  $H$  and  $h$  be the heights of the low-index waveguide at stages I and II, respectively [see Fig. 1(a)]. Let  $\alpha$  be the ratio of heights of the two stages,  $\alpha = H/h$ , determining the amount by which the vertical extent of the mode is reduced by the rib taper. The low-index waveguide has width  $W$  at the beginning of stage I and is narrowed down to  $w$  in the base and  $w_{rib}^{tip}$  in the rib part. It is assumed that the low-index waveguide surrounding the inverse taper has width  $w$  which is constant along the taper. The refractive index of the low-index waveguide is  $n$ .

The values of some coupler parameters have not been subject to optimization and had been fixed in all simulations of this paper. The silicon waveguide (refractive index 3.48) at the output of the coupler is assumed to be 600nm wide and 105nm tall. Such a design, having high aspect ratio, offers low sensitivity to width variations and sidewall roughness [31]. A different silicon waveguide cross-section is only considered in Sec. 6 when discussing polarization dependence. The silicon oxide undercladding (refractive index 1.45) is assumed to be 3.0 $\mu$ m-thick, minimizing the optical leakage into the underlying silicon substrate. The optical wavelength of 1550nm is used everywhere except the finite difference time domain simulations of Sections 4 and 6.

The optimal choice of some coupler parameters is relatively straightforward. The cross-section  $W \times H$  of the low-index waveguide at the coupler's input facet is found from the requirement that the mode mismatch with the optical fiber is minimized. An optimal choice of the input cross-section leads to the mode mismatch loss of about 0.2-0.3dB, assuming that there is no air gap between the fiber and the coupler input facet. In the two-stage coupler, optical losses are possible at locations where the optical structure is discontinuous, i.e. at the points where the rib is terminated, where the inverse Si taper is introduced, and where the low-index structure is terminated and only the Si waveguide remains. To avoid losses at the point where the low-index rib is terminated, the rib tip width  $w_{rib}^{tip}$  must be small enough so that the optical mode is confined mostly in the wider bottom section of the waveguide and is not affected by the termination of the rib. To minimize scattering at the tip of the inverse Si taper, the tip must be narrow enough so that the distortion it introduces to the low-index waveguide is very low and therefore the scattering loss is very low too. In this work, we assumed that the Si tip width is 50nm and the rib tip width  $w_{rib}^{tip} = 0.5\mu$ m. Finally, some optical loss can occur at the end of the coupler where the Si waveguide exits the low-index waveguide. For the Si waveguide cross-section of 600  $\times$  105nm, the loss is around 0.09dB. If this loss needs to be reduced, the Si waveguide outside the coupler can be overcladded with a thin layer ( $\sim 1\mu$ m) of another material such as SiO<sub>2</sub> (not shown in Fig. 1), so that the refractive index discontinuity experienced by the light traveling in the overcladding is minimized. Another solution is to widen the Si waveguide exiting the coupler in order to improve light confinement in the Si core and thus reduce the impact of the overcladding index discontinuity. For example, if the Si waveguide exiting the coupler is not 600nm-wide but 1 $\mu$ m-wide, the loss is reduced from approximately 0.09dB to 0.04dB. We assumed that the losses at the tip of the inverse taper, at the tip of the rib taper, and at the exit from the coupler can be reduced to negligible values, and therefore did not include any of them into consideration in the rest of the paper.

There are also some important coupler parameters the optimization of which needs to be described in more detail. These parameters are the lengths of the two tapers and the height ratio  $\alpha = H/h$ . The coupler design and performance also depends on the refractive index of the low-index waveguide; this dependence will be investigated in the next sections.

We first assume that the cross-sections of the two stages of the coupler are fixed and describe a way to find the optimal lengths of these stages. As an example, consider a coupler with  $W = H = 10\mu$ m,  $w = h = 4.5\mu$ m, and low-index material refractive index  $n = 1.50$ . The

mode conversion losses of the fundamental TE mode in the rib and inverse tapers as a function of length of these tapers are shown in Figs. 2(a) and 2(b). Throughout this work, we consider TE-polarized light only, except in Sec. 6, where the polarization dependence in two-stage couplers is discussed. Unless stated otherwise, the light propagation in the tapered structures was simulated using the eigenmode expansion method, as implemented in the FIMMWAVE/FIMMPROP software package [32].

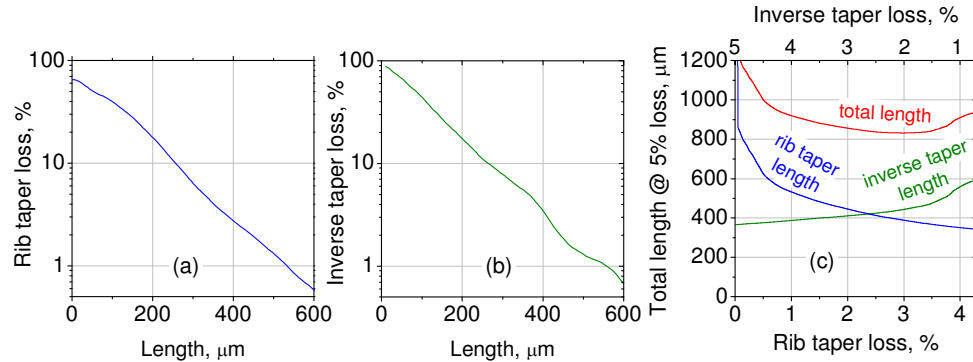


Fig. 2. Optimization of rib and inverse taper lengths for a coupler with  $W = H = 10\mu\text{m}$ ,  $w = h = 4.5\mu\text{m}$ , and  $n = 1.50$ . Plots (a) and (b) show loss vs. length in the rib and inverse tapers. Plot (c) shows rib taper length, inverse taper length, and total length as a function of loss in the rib taper (bottom axis) and inverse taper (top axis), assuming 5% total loss in both tapers.

To minimize the mode conversion loss, the tapers should be made as long as possible. However, making the tapers very long is impractical not only because of chip area restrictions, but also because of other sources of loss that are present in addition to the mode conversion loss. For example, the optical mode experiences scattering due to sidewall roughness of the inverse Si taper. The longer the taper, the higher the scattering loss, therefore increasing the taper length to improve its efficiency does become counterproductive at some point. We selected 5% mode conversion loss as the criterion for designing a coupler which is quite efficient yet reasonably short.

To make a two-stage coupler with 5% mode conversion loss as short as possible, the total loss of 5% should be split between the rib and inverse tapers in a way which minimizes the overall length. Figure 2(c) shows the lengths of the rib taper, inverse taper, and the sum of the two (i.e. the total coupler length) as a function of loss in the rib taper (bottom axis) for our example. The loss in the inverse taper (top axis) is simply 5% minus the loss in the rib taper. We can see that the plot of the total length has a minimum at about 3% loss in the rib taper and 2% loss in the inverse taper. In a similar way, we can find the optimal lengths of the two stages for any given cross-sections of the two stages.

The next step is to choose the optimal value of the height ratio  $\alpha = H/h$ . This parameter controls how much of the total mode area reduction occurs in the rib, and how much in the inverse taper. Larger  $\alpha$  means the mode area is reduced more in the rib taper and less in the inverse taper, therefore the rib taper needs to be longer and the inverse taper can be shortened. This is illustrated in Fig. 3, which shows the lengths required for 5% mode conversion loss in the rib taper [Fig. 3(a)] and inverse taper [Fig. 3(b)] as a function of stage II height  $h$ . In this example, it is assumed that  $W = H = 10\mu\text{m}$ ,  $w = h$ , and refractive index  $n = 1.50$ . The total length of the coupler is the sum of the rib taper length and the inverse taper length, the former increasing and the latter decreasing with  $\alpha$ . One might expect that there exists an optimal height ratio  $\alpha$  which minimizes the total length of the two stages. Figure 4 plots the total length as a function of  $\alpha$ . For each  $\alpha$ , the algorithm described in the previous paragraph has been used to optimize the lengths of the rib and inverse tapers; these optimized values are also plotted in Fig. 4. We can see that the plot of total length versus  $\alpha$  indeed has a minimum, in this example reached for  $\alpha$  around 2.2-3.0. Using this approach we can find the optimum value of  $\alpha$  for any coupler with given input width  $W$ , height  $H$ , and refractive index  $n$ .

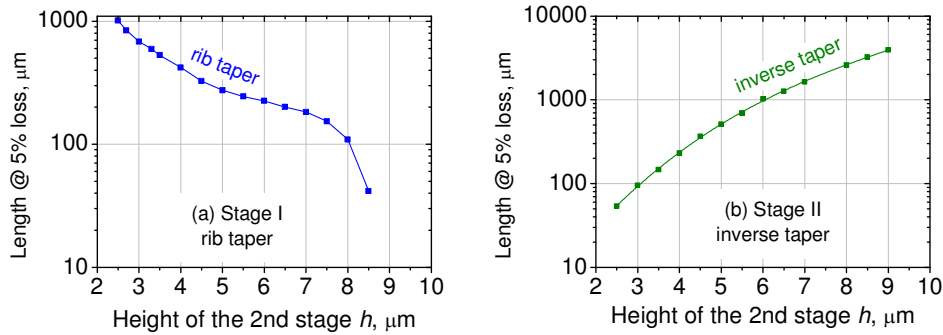


Fig. 3. (a) Length of stage I (rib taper) and (b) length of stage II (inverse taper) as a function of stage II height  $h$ . It is assumed that  $W = H = 10\mu\text{m}$ ,  $w = h$ , and  $n = 1.50$ . The lengths correspond to 5% mode conversion loss.

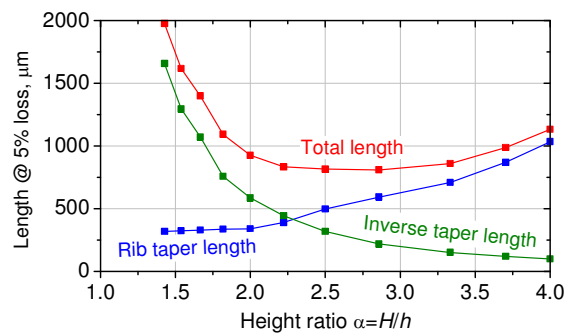


Fig. 4. The total coupler length corresponding to 5% mode conversion loss as a function of height ratio  $\alpha$  for  $H = W = 10\mu\text{m}$ ,  $w = h$ ,  $n = 1.50$ . For each  $\alpha$ , the lengths of the rib and inverse tapers were optimized (the optimal values are also plotted) to minimize the total length.

One important observation in Fig. 3(b) is how fast the length of the inverse taper increases with the height  $h$  of the low-index waveguide. This fast increase is presumably the reason why inverse taper-based couplers developed so far were limited to matching small-core fibers only [3–8]. In our example with low-index waveguide with  $W = H = 10\mu\text{m}$  and  $n = 1.50$ , if an inverse taper only is used to transfer the light into the Si waveguide (i.e.  $w = h = 10\mu\text{m}$ ), the inverse taper length needs to be about 6mm for 5% mode conversion loss. This is too much for most applications. By using the optimized two-stage design, the length can be reduced to about  $800\mu\text{m}$  (Fig. 4), which is already practical for many applications. The proposed two-stage concept therefore allows one to create couplers for fibers with core sizes larger than is possible with pure inverse taper-based couplers.

Also note the fact that there exists a wide range of values of  $\alpha$ , roughly from 2 to 3, over which the coupler design is close to the optimum. Because tall and narrow ribs can be challenging to fabricate, one might prefer to choose a smaller rather than larger  $\alpha$  at the expense of a modest increase in coupler length.

#### 4. Performance of optimized two-stage couplers

This section studies the performance of the optimized two-stage fiber-to-chip couplers as a function of the fiber mode size and the refractive index of the low-index waveguide. The performance of the two-stage couplers is also quantitatively compared to the current state-of-the-art in in-plane couplers, i.e. the couplers based on inverse tapers.

The performance of the inverse and rib tapers depends on the refractive index of the low-index waveguide. To illustrate this, we calculated the length required for 5% mode conversion loss in a rib taper with  $W = H = 4.0\mu\text{m}$ ,  $w = h = 2.0\mu\text{m}$  [see Fig. 1(a) for the notation] and an

inverse taper with  $w = h = 4.0\mu\text{m}$  as a function of refractive index  $n$  (see Fig. 5). We can see that the length of the inverse taper changes considerably with  $n$ , while the length of the rib taper changes only slightly. Therefore, one can expect the dependence of the coupler length on the refractive index to be different for the inverse taper-based coupler and the two-stage coupler, which incorporates both the rib and the inverse taper. To make a valid comparison between the two designs, one needs to make the refractive index a parameter of this comparison.

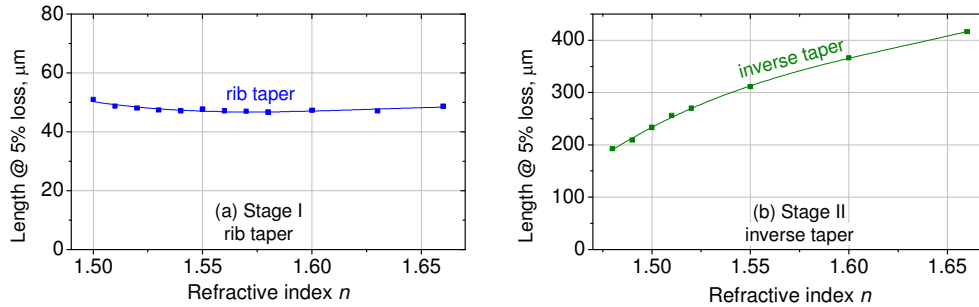


Fig. 5. Dependence of length on refractive index for (a) rib taper with  $H = W = 4\mu\text{m}$ ,  $h = w = 2\mu\text{m}$ , (b) inverse taper with  $w = h = 4\mu\text{m}$ . The refractive index of the  $\text{SiO}_2$  undercladding is 1.45.

To evaluate and compare the performance of the two-stage and the inverse taper-based couplers, we optimized the coupler design for two values of fiber mode field diameter (MFD) and multiple values of low-index waveguide refractive index  $n$ . The values of MFD were  $4.0\mu\text{m}$  and  $8.0\mu\text{m}$ , as defined by the  $1/e^2$  intensity diameter.  $4.0\mu\text{m}$  is the MFD of a small-core fiber, while  $8.0\mu\text{m}$  is a MFD close to the  $10\mu\text{m}$  MFD of a standard single-mode fiber. The optimization results are presented in Figs. 6 and 7. In these figures, the plots on the left correspond to  $\text{MFD} = 4.0\mu\text{m}$ , plots on the right to  $\text{MFD} = 8.0\mu\text{m}$ , and the refractive index  $n$  is the x-axis parameter in all the plots. Figure 6(a) shows the lengths of the two-stage and inverse taper-based couplers matched to the same fiber and having the same mode conversion loss. Figure 6(b) shows the ratio of these two lengths, indicating how much the coupler length can be reduced by switching from the inverse taper-based design to the proposed two-stage design.

For each data point of Fig. 6, the two-stage coupler parameters were optimized as described in the previous section. The optimized parameter values are presented in Fig. 7. The lengths of each section as well as the total length of the two-stage coupler are plotted in Fig. 7(a). The height ratio  $\alpha$  of the optimized designs is shown in Fig. 7(b). One can see that as  $n$  increases, the optimal  $\alpha$  becomes larger, i.e. the role of the rib taper, which has almost index-independent efficiency, becomes more important. This allows the length of the optimized two-stage coupler to be a weaker function of  $n$  than the length of the inverse taper-based coupler.

To minimize the loss at the fiber–low index waveguide interface, the width  $W$  and height  $H$  of the low-index waveguide must be selected to maximize the overlap with the fiber mode. Because the waveguide mode profile depends on its refractive index  $n$ , the values of  $W$  and  $H$  must be adjusted for each value of  $n$  to ensure matching to the fiber. Figure 7(c) shows  $W$  and  $H$  which were used for our two-stage and inverse taper-based designs. According to Fig. 7(c), the waveguide height varies more with refractive index than the width, which happens because the index contrast between the low-index waveguide and  $\text{SiO}_2$  undercladding is relatively low and the mode extends more and more into the undercladding as the refractive index decreases.

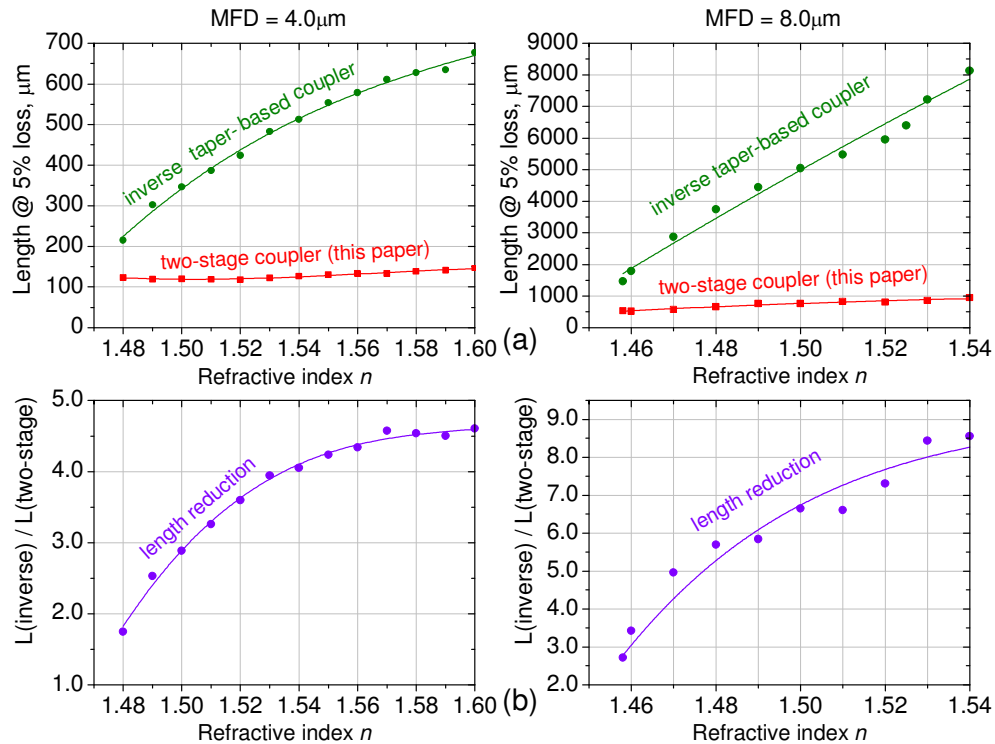


Fig. 6. Performance of the two-stage and inverse taper-based couplers designed for fibers with  $MFD = 4.0 \mu\text{m}$  (plots on the left) and  $8.0 \mu\text{m}$  (plots on the right) as a function of the refractive index  $n$ . (a) Lengths of the optimized two-stage and inverse taper-based couplers with the same input cross-sections and 5% mode conversion loss, and (b) the ratio of these two lengths. The data points represent simulation results, and the curves are the fits to these points. The details of the designs can be found in Fig. 7.

There is one parameter of the two-stage coupler – the width  $w$  of the low-index waveguide in the inverse taper section – which has not been discussed yet. It turns out that the inverse taper length is a much weaker function of width  $w$  than of height  $h$ , as illustrated in Fig. 8. For this reason, instead of performing rigorous optimization of  $w$ , we assumed that the rib taper reduces both the height and the width by the same geometry shrink factor  $\alpha$ , i.e.  $w = W/\alpha$ . There is a concern, however, that for low refractive indices the fundamental mode of the waveguide with  $w = W/\alpha$  and  $h = H/\alpha$  might experience loss due to leakage through the  $\text{SiO}_2$  undercladding. Having a thick enough undercladding is therefore important for efficient operation of low-index two-stage couplers;  $3.0 \mu\text{m}$  thickness is assumed in this work. Still, for large  $\alpha$  and low  $n$  the leakage loss can be non-negligible. To resolve this problem, we adopted the following approach: if the leakage loss for  $w = W/\alpha$  exceeded  $10 \text{ dB/cm}$ , we increased the width  $w$  until the loss was reduced below  $10 \text{ dB/cm}$ . This increase in width  $w$  for large  $\alpha$  means that the inverse taper needs to be longer and therefore the length of the two-stage coupler will increase. This shifts the optimal geometry shrink factor  $\alpha$  to smaller values for low refractive indices. This approach has been used to obtain the results of Fig. 6; the corresponding widths  $w$  are shown in Fig. 7(c) together with heights  $h$  which are always equal to  $H/\alpha$ . Note, that the local substrate removal [33,28] can eliminate the leakage loss altogether and therefore result in better performance of low-index two-stage couplers.

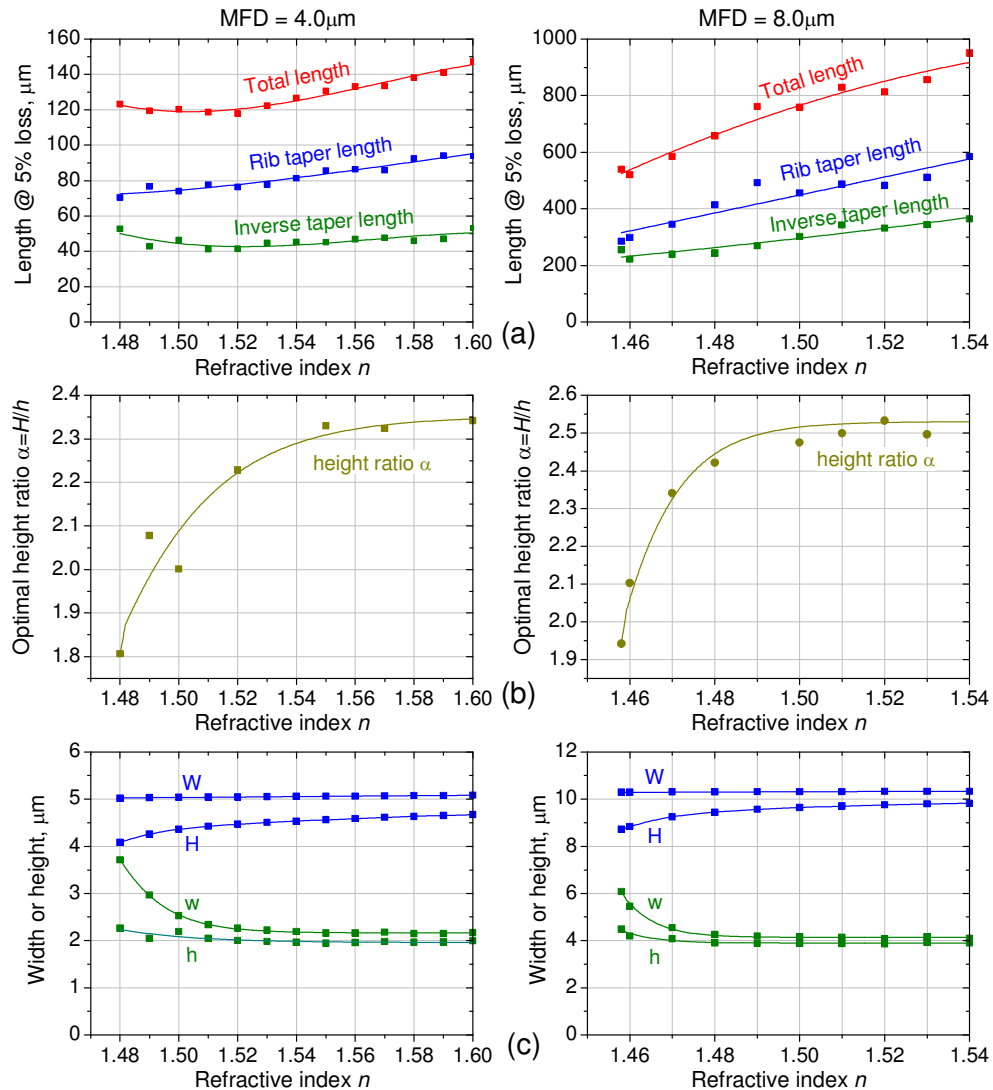


Fig. 7. Parameters of the optimized two-stage couplers whose lengths are plotted in Fig. 6. The fiber MFD is 4.0 μm and 8.0 μm for the left- and the right-hand plots, respectively, and the coupler parameters are plotted as a function of refractive index  $n$ . (a) Lengths of the inverse taper section, rib taper section, and the total length of the optimized two-stage coupler with 5% mode conversion loss; (b) the height ratio  $\alpha$  of the optimized two-stage coupler; (c) width  $W$  and height  $H$  of the low-index waveguide at the input where it matches the fiber, as well as width  $w$  and height  $h$  of the low-index waveguide in the inverse taper section. The data points represent simulation results, and the curves are the fits to these points.

One observation with respect to the simulation results that is worth addressing is that the plots of some of the data are not entirely smooth (see Figs. 6, 7 as well as Figs. 3–5). This is because the underlying dependence of mode conversion loss on taper length is typically not a perfectly smooth function but exhibits some oscillations due to phase-dependent energy exchange between the fundamental and multiple higher-order modes. This energy exchange occurs because pushing these designs to shorter lengths means a departure from entirely adiabatic behavior, and a need to deal with some degree of mode coupling. For example, consider the last three points ( $n = 1.58, 1.59, 1.60$ ) of the inverse taper length plot for MFD = 4.0 μm [left plot in Fig. 6(a)], which are irregularly spaced along the y-axis. Figure 9 shows

how the mode conversion loss depends on taper length for these three refractive indices. We can observe that the loss decays with length in somewhat irregular way [see also Figs. 2(a), (b)], and sometimes the curves in Fig. 9 even intersect. As a result, the length shown in Fig. 6(a) is not a perfectly smooth function of the refractive index. The oscillations are especially visible in Fig. 7(b) showing the optimal height ratio  $\alpha$ . However, these oscillations are not a problem because the range of  $\alpha$  for which the coupler performance is very close to the optimum is quite wide (see Fig. 4). Despite some oscillations, the general trend of all plots in Figs. 3–7 is stable.

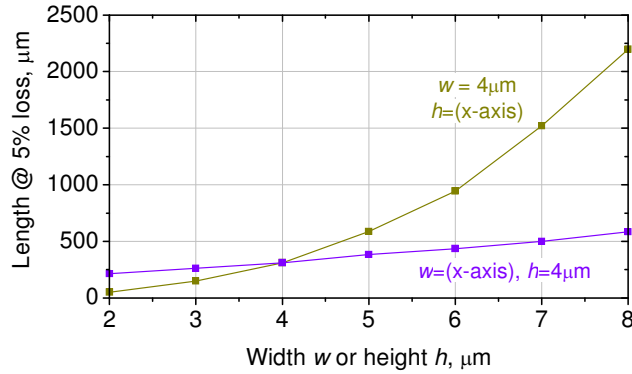


Fig. 8. Dependence of inverse taper length on width  $w$  and height  $h$  of the low-index waveguide with  $n = 1.55$ . For one curve, the width is  $4\mu\text{m}$  and the height is the x-axis parameter, and for the other curve, the height is  $4\mu\text{m}$  and the width is the x-axis parameter.

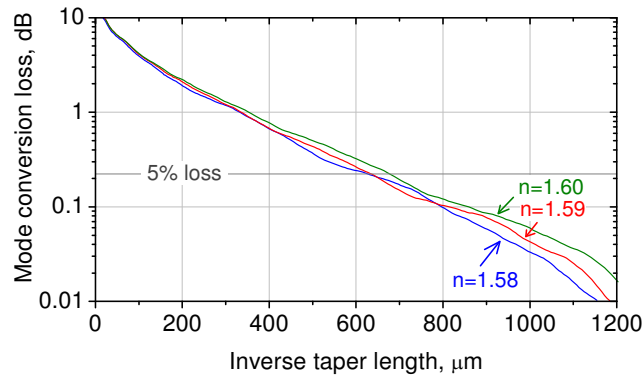


Fig. 9. Mode conversion loss as a function of length of an inverse taper-based coupler matched to a fiber with  $\text{MFD} = 4.0\mu\text{m}$  for  $n = 1.58, 1.59, \text{ and } 1.60$ . The last three points in the upper line in the left plot of Fig. 6(a) are given by intersection of the three curves of Fig. 9 with the 5% loss line.

All coupler simulations described in this and the previous sections were carried out with the eigenmode expansion method [32], which allows relatively quick simulation of the light propagation in tapers. Once the output for one taper length is evaluated using this method, the output for any other length can be obtained almost instantaneously, which has been very valuable for the taper optimizations performed in this paper. However, the accuracy of the eigenmode expansion method depends on the number of modes included in the simulation, and in practice this number is limited. To verify that the accuracy of our eigenmode expansion simulations was sufficient, we performed a rigorous finite-difference time-domain (FDTD) simulation for one of the coupler designs.

Figure 10(a) shows the mode conversion loss calculated with FDTD method for one of the two-stage coupler designs from Figs. 6, 7. The design selected for these simulations was for the coupler matched to a fiber with  $\text{MFD} = 4.0\mu\text{m}$  with the refractive index of the low-index

waveguide  $n = 1.55$ . The lengths of the rib taper section, inverse taper section, and the total length were  $85.5\mu\text{m}$ ,  $45.1\mu\text{m}$ , and  $130.6\mu\text{m}$ , respectively. The low-index waveguide dimensions were  $W = 5.05\mu\text{m}$ ,  $H = 4.56\mu\text{m}$ ,  $w = 2.15\mu\text{m}$ ,  $h = 1.95\mu\text{m}$ , and  $w_{rib}^{tip} = 0.5\mu\text{m}$  (see Fig. 1 for notation), the silicon waveguide cross-section was  $50 \times 105\text{nm}$  at the beginning and  $600 \times 105\text{nm}$  at the end of the inverse taper. Similar to all coupler designs presented in Figs. 6, 7, this design was optimized for 5% (0.22dB) mode conversion loss for TE-polarized light. FDTD simulation predicts 0.17-0.18dB loss [Fig. 10(a)], confirming the validity of using the eigenmode expansion method for coupler optimization.

For comparison, the mode conversion loss in a pure inverse taper-based coupler of the same length and input cross-section was also calculated with FDTD method. The results are shown in Fig. 10(b). As expected, the pure inverse taper-based coupler of this length does not perform well, having about 10 times larger loss than the optimized two-stage coupler.

Notice that the two-stage coupler is very broadband, with very little efficiency variation over the simulated wavelength range of 100nm [Fig. 10(a)]. This was to be expected from a device based on the principle of adiabatic mode evolution.

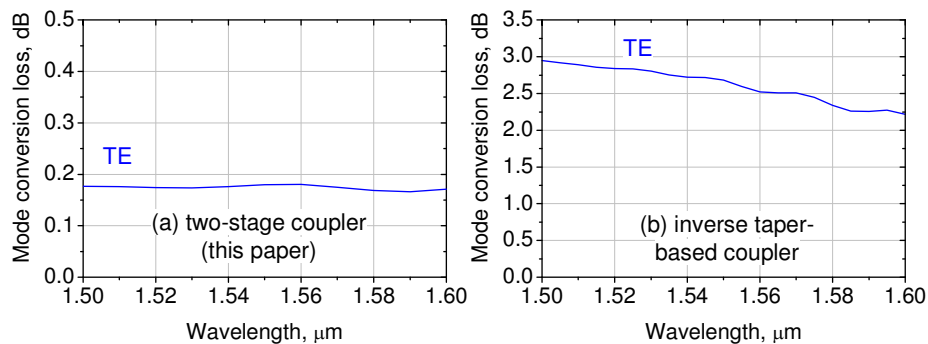


Fig. 10. The loss in (a) an optimized two-stage coupler and (b) an inverse taper-based coupler of the same length, obtained with 3D FDTD simulations. The couplers were matched to a fiber with MFD =  $4.0\mu\text{m}$ , the total length was  $130.6\mu\text{m}$ , and the low-index waveguide had  $n = 1.55$ . The two-stage coupler was optimized for 5% (0.22dB) mode conversion loss at  $1550\text{nm}$  with the eigenmode expansion method [32].

## 5. Choice of refractive index of the low-index waveguide

As mentioned in the previous section, the performance of both the proposed two-stage couplers and inverse taper-based couplers depends on the refractive index of the low-index waveguide. Now, we would like to discuss the choice of refractive index in more detail.

In general, it is better to choose a lower value of refractive index  $n$  for both the two-stage and the inverse taper-based designs. This is true for two reasons, one being that the coupler length decreases as  $n$  becomes lower, especially in the case of pure inverse taper-based couplers. The second reason is that as  $n$  increases, the low-index waveguide at the coupler input turns from a single- into a multi-mode regime. In the two examples with MFD =  $4.0\mu\text{m}$  and  $8.0\mu\text{m}$  discussed in the previous section (see Figs. 6 and 7), the transition into multi-mode regime happens at  $n = 1.485$  and  $n = 1.459$ , respectively. It is often desirable to stay away from the multi-mode regime because of the possibility of multi-mode effects in the coupler. However, while a lower refractive index  $n$  is preferred, it should not be too low for three reasons: (1) if  $n$  is too low, the fundamental mode leaks through the  $\text{SiO}_2$  undercladding into the Si substrate; (2) the length of the two-stage coupler might actually increase when it becomes necessary to widen up the inverse taper stage for low values of  $n$ , as discussed in the previous section; (3) as  $n$  becomes lower, the index contrast with the undercladding is reduced, the fundamental mode becomes asymmetric, and the mode mismatch with the fiber increases. We did not perform rigorous optimization of coupler performance which considers the impact of leakage loss of the fundamental mode and the increased mismatch with the fiber

in case of low refractive indices. However, if the refractive index is chosen at the 2nd mode cutoff, i.e. if the refractive index is not too low while the coupler is still single-mode, the factors (1)-(3) mentioned above should not be significant and the coupler performance should be close to optimal. In our examples with  $MFD = 4.0\mu\text{m}$  and  $8.0\mu\text{m}$ , the refractive indices  $n = 1.485$  and  $n = 1.459$  should therefore give close-to-optimal performance. For these refractive indices, the two-stage design allows a reduction of the coupler length compared to the inverse taper-based design approximately by a factor of 2 and 3 for  $MFD = 4.0\mu\text{m}$  and  $MFD = 8.0\mu\text{m}$ , respectively.

However, it is not always possible to operate the low-index waveguide in the single-mode regime. This may happen because it might be difficult to select a material which has the specific value of refractive index necessary for optimum coupler performance and at the same time is compatible with existing fabrication processes and has the desired physical properties. Even if such a material is available, it might happen that the exact value of its refractive index cannot be controlled precisely enough, i.e. it is difficult to make sure that the refractive index of the fabricated waveguide is equal to the given pre-defined value in a reproducible way. Especially sensitive to refractive index variations are couplers designed for large mode field diameter fibers. In our example of the single-mode coupler with  $MFD = 8\mu\text{m}$  and  $n = 1.459$ , an error in refractive index of 0.01 will cause the fundamental mode to be cut-off. To be on the safer side and make sure the coupler will function even if the refractive index turns out to be lower than expected, one may choose to use a material with a higher nominal refractive index value, in which case the coupler will operate in a multi-mode regime. For multi-mode couplers, the advantage of the two-stage design over inverse taper-based designs is especially high, as shown in Fig. 6(b).

If the low-index waveguide of the coupler is multi-mode, in principle this does not necessarily lead to problems. If the quality of fabrication is high enough, i.e. the imperfections such as sidewall roughness are low, there will be no energy exchange between the modes as they travel along the coupler because the effective mode coupling will be insufficient to overcome their propagation constant mismatch. If some of the higher-order modes happen to be excited due to misalignment of the input fiber, they will just radiate away at the end of the coupler and only the fundamental mode will be adiabatically coupled into the single-mode Si waveguide. However, if the fabrication quality is not high enough, the coupling coefficients between the fundamental and the higher-order modes may be non-zero so that the modes will exchange energy as they propagate along the taper and the transmission spectrum of the coupler will exhibit oscillations. Depending on the magnitude of fabrication errors, these oscillations might be severe enough to render the coupler unusable. Nevertheless, if the fabrication quality is high, as can be expected from today's photonic fabrication processes [34,35], so that the coupling between the modes is negligible, the two-stage design gives much more freedom in the choice of refractive index because its performance is not nearly as index-dependent as that of the inverse taper-based design [see Fig. 6(a)]. This significantly broadens the range of materials that can be used for fabrication of the low-index waveguide.

## 6. Polarization dependence

The designs presented in the previous sections were optimized for TE-polarized light; the TM polarization was not considered. Couplers working only with TE polarization are useful for many applications, such as intra- and inter-chip communications and on-chip photonic analog-to-digital conversion, when the optical integrated circuits work with TE polarization only and the TM-polarized light is not used. However, in other applications, such as in fiber optics, polarization-independent coupler performance is essential [30]. Although we did not perform a rigorous study of the two-stage couplers for TM-polarized light, we predict that the two-stage design will be efficient in this case as well.

To confirm that the two-stage concept is efficient also for TM light, we selected one coupler design and performed FDTD simulations for both polarizations. In previous sections, we considered silicon waveguides with  $600\times 105\text{nm}$  cross-section which was optimized for TE light and had poor confinement of the TM mode. To make sure the TM mode is well-confined

in the Si core, we increased the waveguide thickness to 220nm. Assuming that the input fiber has MFD = 4.0 $\mu$ m and the low-index waveguide has  $n = 1.55$ , we optimized the two-stage coupler design for TE light using the algorithm described in the previous sections. The lengths of the rib taper section, inverse taper section, and the total length were 85.2 $\mu$ m, 43.2 $\mu$ m, and 128.4 $\mu$ m, respectively. The low-index waveguide dimensions were  $W = 5.06\mu\text{m}$ ,  $H = 4.56\mu\text{m}$ ,  $w = 2.16\mu\text{m}$ ,  $h = 1.96\mu\text{m}$ ,  $w_{rib}^{tip} = 0.5\mu\text{m}$ , and the Si waveguide was 50nm wide at the beginning and 440nm wide at the end of the inverse taper. According to the eigenmode expansion method, this TE-optimized design gives 5% (0.22dB) mode conversion loss at 1550nm.

The results of FDTD simulations are shown in Fig. 11(a). One can see that although the coupler was optimized for TE-polarized light, it performs quite well also for the TM polarization. For comparison, the loss in the pure inverse taper-based coupler of similar length and input cross-section was calculated, see Fig. 11(b). This loss is several times higher than for the two-stage design.

One detail to keep in mind when designing a polarization-independent two-stage coupler is that for low refractive indices the leakage through the SiO<sub>2</sub> undercladding is higher for TM than for TE-polarized light. Therefore, for small refractive indices, the height ratio  $\alpha$  might need to be reduced to make the coupler work efficiently for both polarizations.

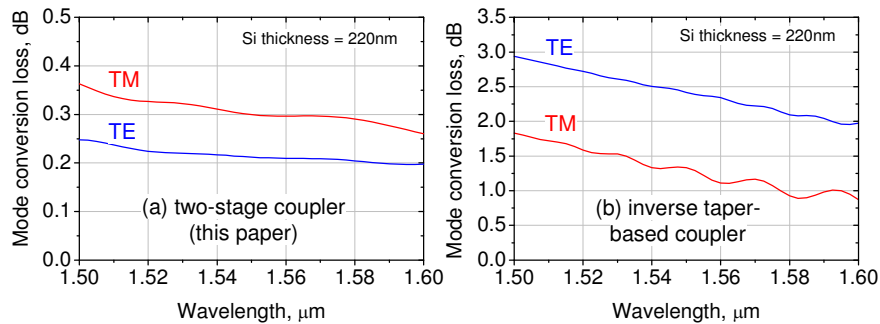


Fig. 11. The loss in (a) an optimized two-stage coupler and (b) an inverse taper-based coupler obtained with three-dimensional FDTD simulations. The input fiber had MFD = 4.0 $\mu$ m, the total length was 128.4 $\mu$ m, and the low-index waveguide had  $n = 1.55$  for both cases. Compared to the other simulations in this paper, the silicon waveguide thickness was increased from 105nm to 220nm to improve the confinement of the TM mode.

## 7. Summary and conclusions

In this work, we propose a new design of an adiabatic in-plane fiber-to-chip coupler which consists of two stages, a rib taper and an inverse taper. This design is compatible with planar fabrication technology and does not require to use such fabrication techniques as gray-scale lithography. Because the coupler operation is based on the principle of adiabatic mode evolution, its performance is broadband and is expected to be tolerant to fabrication errors.

The proposed two-stage design allows to reduce coupler length as compared to the state-of-the-art couplers based on inverse tapers with the same mode conversion efficiency. The magnitude of length reduction depends on the refractive index of the low-index material of the coupler and mode size of the fiber for which the coupler is designed. If the low-index waveguide is single-mode, the length of the couplers matched to fibers with MFD = 4.0 $\mu$ m and 8.0 $\mu$ m is reduced 2- and 3-fold, respectively. If the refractive index is higher, e.g. because no material with the required low index is available in the given fabrication process, the advantage of the two-stage design is even larger, enabling length reduction of up to about 4.5-fold for MFD = 4.0 $\mu$ m and even more for MFD = 8.0 $\mu$ m, depending on the exact value of the refractive index. However, the use of higher refractive index implies that the fiber-matched

waveguide is multi-mode, in which case the fabrication quality must be high enough to avoid power exchange between the modes propagating along the coupler.

To achieve high efficiency in a two-stage coupler, one needs to optimize the cross-section of the fiber-matched waveguide, the lengths of the rib and inverse tapers, the height ratio  $\alpha$ , as well as some other parameters. The optimization procedure is described in Sec. 4. For our two examples with MFD = 4.0 $\mu\text{m}$  and 8.0 $\mu\text{m}$ , the optimal values of  $\alpha$  were between 2 and 3. It was found that the performance of the coupler is close to optimal within a quite wide range of  $\alpha$  so that the precise value of  $\alpha$  is not very important. For low refractive indices, care must be taken to avoid optical loss due to leakage of the fundamental mode through the oxide undercladding. The leakage loss can be reduced by limiting  $\alpha$  and widening the low-index waveguide in the inverse taper section.

The increased conversion efficiency offered by the two-stage coupler means that the footprint of the coupler on a chip can be reduced. Importantly, this also means that for a given footprint, the two-stage design can work with fibers with increased mode size. The increased fiber mode size leads to improved misalignment tolerances and simplified chip packaging. In addition, if a lensed fiber is used to bring light to the chip, a larger focal spot size usually means lower insertion loss because the lensed fiber losses are strongly spot size-dependent.

It is necessary to note that while in this work we were mostly discussing the mode conversion loss, there may be also other sources of loss in the coupler, such as the loss due to mode mismatch with the fiber (0.2-0.3dB). Therefore, whenever it is mentioned that a coupler has a mode conversion loss of 5% (0.22dB), it is necessary to keep in mind that the total loss of such a coupler is approximately 0.5dB. Additional losses at locations where the rib taper ends, inverse taper starts, and the low-index waveguide overlaying the inverse taper is terminated can be avoided with proper design.

Another source of loss is the scattering loss induced by the sidewall roughness of the inverse Si taper. For given roughness, scattering losses increase as the waveguide becomes narrower [36], therefore the roughness-induced loss in the inverse taper will be higher than in a full-width Si waveguide of the same length. We did not consider the scattering-induced loss because it is determined by the fabrication quality and can in principle be reduced to a very low value as fabrication techniques are being improved. Even if this loss is high, e.g. 20dB/cm, the total loss in the inverse taper of the two-stage coupler is only around 0.1dB for MFD = 4.0 $\mu\text{m}$  and 0.5dB for MFD = 8.0 $\mu\text{m}$  for the designs of Fig. 7. Note that compared to pure inverse taper-based couplers, the scattering loss in two-stage couplers is lower because their length is shorter and because the inverse taper occupies only a part of this length.

Although all optimizations in this work were carried out for TE-polarized light, we predict that the two-stage coupler concept is efficient for TE and TM polarizations simultaneously. This was confirmed with FDTD simulations for one example of a coupler design. In this example a Si waveguide with thicker core – 220nm rather than 105nm as in the rest of the paper – has been assumed. Efficient operation of the two-stage coupler in this case illustrates that the two-stage design can be efficient for different Si waveguide geometries.

The couplers in this paper were designed assuming linear taper shapes in the two stages. Initial results on optimized taper shapes show that switching from a linear to an optimized taper shape allows to gain a factor of 2-3 in length, which is in addition to the gain achieved by switching from the conventional inverse taper-based design to the two-stage design. This additional improvement in coupler efficiency should make it possible to practically couple light directly from standard single-mode fibers with 10 $\mu\text{m}$  mode field diameter. This subject requires further investigation.

### Acknowledgements

This work was sponsored by the DARPA EPIC Program under contract W911NF-04-1-0431.